Demand Response in Smart Districts: Model Predictive Control of Building Cooling

Philipp Zwickel, Moritz Frahm, Johannes Galenzowski,
Karl-Heinz Häfele, Heiko Maaß, Simon Waczowicz, and Veit Hagenmeyer
Karlsruhe Institute of Technology, Institute for Automation and Applied Informatics, Karlsruhe, Germany
philipp.zwickel@kit.edu

***Abstract*—The present paper develops and compares three different Model Predictive Control (MPC) strategies for Demand Response (DR) of building cooling in a "smart district": Decentralized MPC (DeMPC), Centralized MPC (CeMPC), and scheduled Distributed MPC (DiMPC). A standard DeMPC approach leads to peaks in aggregated cooling power demand, as local controlling agents optimize each building decentrally. Because these peaks can stress the local power grid severely, we present and compare two additional MPC approaches, CeMPC and DiMPC, to enforce a constraint on the aggregated power use of the district. Our simulation results show that CeMPC and scheduled DiMPC reduce the peak load of the total cooling power in the district by 50 % while still providing DR and cooling the buildings adequately.**

***Index Terms*—demand response, smart district, model predictive control (MPC), scheduling, building cooling**

I. Introduction

The energy demand for cooling appliances increases for the main share of European countries, partly due to temperature increases from climate change. Larsen et al. [1] point out that the cooling demand in 2050 will increase in the range of $25\,\%$ to $50\,\%$ relatively to 2010. A portion of countries will exceed a doubling in cooling demand during this period [1]. This significant demand increase adds burdens to the power grid. As a key solution to reduce this burden, Demand Response (DR) programs could balance the load of cooling appliances and thus stabilize the power grid.

In that context, Model Predictive Control (MPC) offers the large potential to provide DR while maintaining thermally comfortable conditions for the occupants inside buildings. This model-based control strategy defines an optimal input trajectory as it accounts for future predictions of system dynamics, weather forecasts, occupants' demands, and electricity prices [2]. In addition, MPC can consider sets of constraints for output and input limitations, e.g. due to thermal boundaries or technical limitations. MPC can be applied for Heating, Ventilation, and Air Conditioning (HVAC) systems of single buildings or for entire building districts.

In the present work, we develop an MPC strategy for building cooling in a smart district. In this context, the following paragraphs present existing work about MPC for smart district cooling with different approaches, centralized vs. decentralized MPC, and the handling of power limitations on a district level.

Related work about MPC in the context of district cooling mainly focuses on coupling over local cooling networks and on the control of a single building. Coccia et al. [3] evaluate a single building with an MPC in a local cooling network with thermal energy storage and variable-load heat pumps. As only a single building is evaluated, electrical coupling effects between buildings are not considered. In contrast, Buffa et al. [4] couple building cooling with a district cooling network, but individual cooling for each building is not considered. Similarly, Ma et al. [5] examine a single building and implement a price-based demand response. Ma et al. [5] state that MPC is highly suited for pre-cooling and shifting load from peak hours. While most literature in the context of district building cooling evaluates single buildings and local cooling networks, the present paper considers district-level control of individual building cooling, where we couple the buildings over the electrical grid.

On the district level, the buildings' loads need to comply with global limits such as peak power demand. Therefore, MPC can coordinate the different buildings with one of three different MPC architectures: 1. decentralized, 2. centralized, or 3. distributed MPC.

1. **Decentralized MPC (DeMPC)**: Each building has its MPC, which does not take any interdependency with the other buildings into account.
2. **Centralized MPC (CeMPC)**: The MPC calculates the full optimization problem and explicitly accounts for global constraints and coupling conditions.
3. **Distributed MPC (DiMPC)**: The coordination is done globally, while the main computational effort is distributed among the individual subsystems.

Mork et al. [6] compared these three different MPC approaches on the single-building level, with a multi-zone building model. In that case, each room is considered as one subsystem to be optimized. In addition, the authors compare the three MPC approaches to rule-based control and PI control. They found out that 1) the distributed MPC approach outperformed the centralized, and 2) that a decentralized approach is a suitable approach to account for global limitations. According to Mork et al. [6], future work could include up-scaling of the system to larger systems and the integration of additional coupling constraints. Consequently, the next step involves the investigation of the various MPC approaches on the district

level, as we address in the present work. The main difference between the present work and previous [6] is that we consider an entire district with multiple buildings as a central system with the individual buildings as the subsystems, whereas Mork et al. [6] describe a single building as the central system and the rooms as subsystems.

Unlike Mork et al. [6], other authors evaluate the potential of an entire district but only for the decentralized approach, such as El Geneidy and Howard [7] and Pflaum et al. [8]. El Geneidy and Howard [7] focus on a decentralized approach and the analysis of the influence of varying boundary conditions. The aim of their study was to identify the key characteristics that affect the energy flexibility potential of smart districts. Pflaum et al. [8] also evaluate the decentralized approach for the following three reasons: safety, privacy, and computational costs (due to large problem sizes in a centralized approach). Despite the missing comparison to a centralized approach, El Geneidy and Howard [7] state that centralization can achieve efficient and sustained demand reduction in districts with high variability in usage patterns and thermal characteristics.

Decentralized approaches without a coordinating mechanism can lead to the violation of power limits through synchronized responses of the individual customers, leading to new demand peaks. To prevent these synchronized response peaks, control algorithms can coordinate the load within the district. In the case of district cooling systems, the MPC can limit the pumping power [9]. In contrast, when the cooling units in a district are coupled over the electrical grid, it is possible to constrain the shared electrical power limit of a common substation of the smart district.

Despite the high importance of reducing peak load, we found limited research on the reduction of synchronized peak load from DR with MPC in building cooling. In the present work, we answer the **research question**: How can we limit peak load due to synchronized behavior of DR with MPC in building cooling? Therefore, we compare the peak-limiting capabilities of a Centralized MPC (CeMPC) and a Distributed MPC (DiMPC) scenario with the uncoordinated case of a Decentralized MPC (DeMPC) scenario.

II. MPC for DR in Smart districts

In the following, we describe the three different MPC scenarios shown in Figure 1: 1. DeMPC, 2. CeMPC, and 3. DiMPC. In the 1. DeMPC scenario, we formulate and solve separate MPC problems for each building, that all receive equal price signals. Thus, we cannot consider the maximum grid power constraints of the local power grid, since the individual MPCs have no communication with each other. In the 2. CeMPC, we formulate and solve one global optimization problem for all buildings and the local power grid. The price signal is equal to the first scenario. In the 3. scheduled DiMPC scenario, we formulate separate MPC problems for each building and additionally use a scheduler, which communicates with the individual MPCs. This communication ensures that the local grid constraints are enforced by using the predicted demand of each building to design a schedule that respects the local power grid constraints. This schedule is sent back to the different buildings' MPCs. Finally, the individual MPCs can account for their constraints on power in advance and react accordingly.

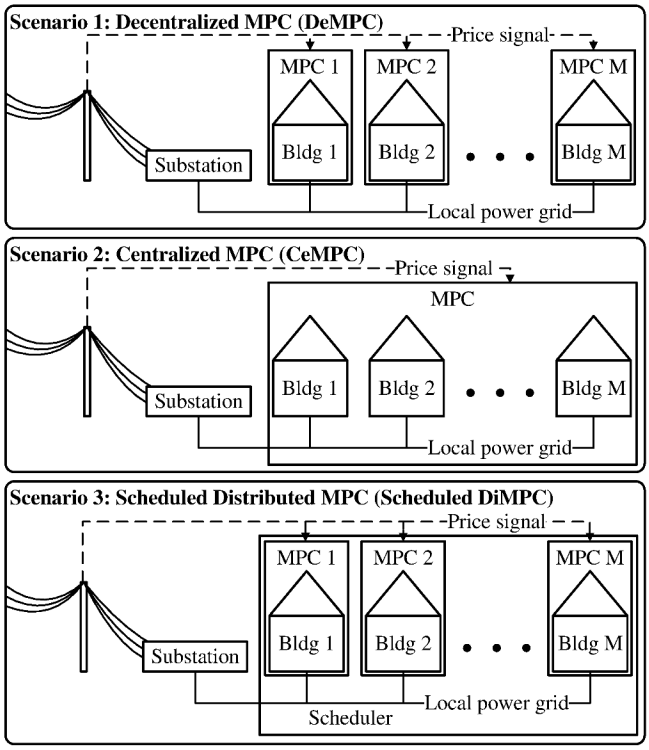

Fig. 1: Overiew of the three different MPC scenarios.

A. Optimization Problem

In all three scenarios, we use discrete-time state-space notation to formulate the respective optimal model predictive control problems. Mathematically, we formulate the respective optimal control problems at time t with a prediction horizon of N time steps based on [10], [11]:

$$\min_{u(\cdot|t)} \sum_{k=t}^{t+N-1} l\left(k, y(k|t), u(k|t)\right) \tag{1a}$$

$$\text{subject to} \forall k \in [0, N-1]:$$

$$x(k+1|t) = A_{\mathrm{d}} x(k|t) + B_{\mathrm{d}} u(k|t) + E_{\mathrm{d}} z(k|t) \tag{1b}$$

$$y(k|t) = C_{\mathrm{d}} x(k|t) \tag{1c}$$

$$x(0|t) = x(t),\ u(k|t) \in \mathcal{U},\ y(k|t) \in \mathcal{Y} \tag{1d}$$

where $l\left(k, \cdot, \cdot\right)$ is the stage-cost, (1b) and (1c) are the discrete-time model, (1d) is the initial condition. $x(t)$ is typically measured at the time t, and $\mathcal{U}$ as well as $\mathcal{Y}$ are input and output constraint sets. The k-step ahead prediction for the states, inputs, disturbances, and outputs based on the current initial condition are denoted by $x(k|t)$, $u(k|t)$, $z(k|t)$, and $y(k|t)$, respectively.

B. Thermal District Model

In this section, we describe how to model the electro-thermal dynamics of a smart district as required for the MPC in Eq. (1). The controller uses a Linear Time-Invariant (LTI) differential equation system in state-space representation,

$$\begin{aligned} \dot{x} &= f(x,u,z) = Ax + Bu + Ez, \\ y &= g(x) = Cx, \quad x_0 = x(0), \end{aligned} \tag{2}$$

where x describes the temperature states of the buildings' envelope and air, u the control inputs, z the measurable disturbances, and y the control output (see Tab. I):

$$x = (T_{\text{air}}\ T_{\text{w}})^{\mathsf{T}},\ y = T_{\text{air}},\ u = \Phi_{\text{c}},\ z = (\phi_{\text{global}}\ T_{\text{amb}})^{\mathsf{T}}. \tag{3}$$

TABLE I: Variables of state-space model

Control var.	Phys. var.	Definition	Unit
state x_1, output y	T_{air}	indoor air temperature	°C
state x_2	T_{w}	wall temperature	°C
input u	Φ_{c}	heat flow of cooling	W
disturb. z_1	ϕ_{global}	global solar radiation	W m^{-2}
disturb. z_2	T_{amb}	ambient air temperature	°C

For a convenient and physically illustrative model, we apply the Resistor–Capacitor (RC) analogy, which simplifies the laws of thermodynamics and heat transfer into a linear representation [12]:

$$\Phi(t) = \frac{T_{\text{a}}(t) - T_{\text{b}}(t)}{R}, \quad C\frac{\mathrm{d}T(t)}{\mathrm{d}t} = \Phi_{\text{in}}(t) - \Phi_{\text{out}}(t). \tag{4}$$

Based on our previous work [13], we present our resulting thermal building model (see Fig. 2), which contains three input variables: the solar radiation Φ_{sol}, the cooling Φ_{c}, and the ambient temperature T_{amb}. All inputs directly affect the indoor air temperature T_{air}. This temperature is also connected to the wall temperature node T_{w}.

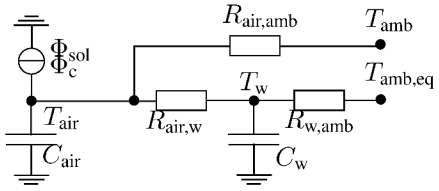

Fig. 2: RC building model

The wall's outside is connected to the equivalent ambient temperature $T_{\text{amb,eq}}$ that also accounts for solar radiation ϕ_{global}. The solar additionally affect the inside air temperature by the heat flow Φ_{sol}, which consists of the global radiation ϕ_{global} and the solar heat gain factor f_{sol} [14].

$$T_{\text{amb,eq}} = T_{\text{amb}} + \phi_{\text{global}} \cdot \frac{a_{\text{f}}}{\alpha_{\text{A}}}, \quad \Phi_{\text{sol}} = f_{\text{sol}} \cdot \phi_{\text{global}} \tag{5}$$

Each temperature is a dynamic state x, characterized by its connected capacitor C as described by the corresponding differential equations (6) and (7):

$$C_{\text{air}}\frac{\mathrm{d}T_{\text{air}}}{\mathrm{d}t} = \frac{T_{\text{w}} - T_{\text{air}}}{R_{\text{air,w}}} + \frac{T_{\text{amb}} - T_{\text{air}}}{R_{\text{air,amb}}} + \Phi_{\text{sol}} + \Phi_{\text{c}} \tag{6}$$

$$C_{\text{w}}\frac{\mathrm{d}T_{\text{w}}}{\mathrm{d}t} = \frac{T_{\text{air}} - T_{\text{w}}}{R_{\text{air,w}}} + \frac{T_{\text{amb,eq}} - T_{\text{w}}}{R_{\text{w,amb}}} \tag{7}$$

For the thermal parameter identification, we use Matlab's "Identification" toolbox [15] and the "greyest" function. This grey-box modeling technology requires a state-space model, as previously described, and measurement data of input and output. Each subsystem is identified individually, similarly to a decentralized multi-zone grey-box model [16].

C. Scenario Development

While in scenarios 1 and 3 the discrete-time models used for each MPC only describe the thermal dynamics of the respective building, the discrete-time model used in the CeMPC in scenario 2 describes the thermal dynamics of all buildings. Naturally, this means that in scenario 2 $x(k|t)$, $u(k|t)$, $z(k|t)$, and $y(k|t)$ are vectors containing the states, inputs, disturbances, and outputs of all buildings, respectively.

In all three scenarios, we consider the following stage cost

$$l(k,y,u) = p(k)^T u_p(k) + w_\xi(\xi(k)^T\xi(k)), \tag{8}$$

where $p(k)$, $k \in \{t : t+N-1\}$, is a time-dependent price signal that represents time-varying prices with $p(k) \in (0,1)$, $u_p(k) = u(k)/P_{\text{nom}}$, $k \in \{t : t+N-1\}$ with $0 \leq u_p(k) \leq 1$ is the percentage of nominal power of the cooling system P_{nom} used. $w_\xi = 10000$, is a penalty factor for the slack variable $\xi(k)$, $k \in \{t : t+N-1\}$ with $0 \leq \xi(k)$.

The first term in (8) shapes the power demand of the building according to the price signal, meaning it penalizes power demand stronger if the prices are higher, thus allowing for DR. Furthermore, the price signal encourages energy consumption at times of lower prices which hints at an overproduction of electricity, e.g. due to renewables. The second term penalizes the slack variable ξ when the outputs are not in the desired temperature range, thus providing a certain level of thermal comfort to the occupants.

Moreover, there are some physical and regulatory constraints we have to consider. Based on [11], we use physical quantities in the following and define

$$\mathcal{Y} = \{y \in \mathbb{R} \,|\, 19\,°\text{C} - \xi \leq y \leq 23\,°\text{C} + \xi\} \tag{9}$$

as a soft constraint for the output, keeping the air temperature inside the building in a temperature range of about $\pm 2\,\text{K}$ around the desired temperature of $21\,°\text{C}$ using the slack variable ξ. Furthermore, the cooling systems are constrained by their physical limitations and the local grid. Since all three scenarios handle the local grid constraints differently, we define the corresponding input constraints as

$$\mathcal{U} = \{u \in \mathbb{R} \,|\, u = u_p * P_{\text{nom}} \wedge 0 \leq u_p \leq 1\} \tag{10a}$$

$$\mathcal{U} = \{u \in \mathbb{R} \,|\, u = u_p * P_{\text{nom}} \wedge 0 \leq u_p \leq 1 \wedge \sum u \leq u_{\text{grid}}\} \tag{10b}$$

$$\mathcal{U} = \{u \in \mathbb{R} \,|\, u = u_p * P_{\text{nom}} \wedge 0 \leq u_p \leq 1 \wedge u \leq u_{\text{sched}}\} \tag{10c}$$

where P_{nom} is the nominal power of the cooling system, u_{grid} is the grid capacity and u_{sched} is a limit given by the scheduler. The values of the nominal power of the cooling systems P_{nom} of the different buildings can be found in Table II. Using the stage cost (8) we perform an economic optimization considering time-varying prices to provide DR.

TABLE II: Construction year and nominal cooling power P_{nom} in kW of the considered buildings.

Bldg. i	1	2	3	4	5	6	7	8	9
Year	1981	1973	1973	1980	1969	2011	2015	2008	2018
P_{nom}	190	180	250	180	170	250	540	1000	230

D. Scheduling

In scenario 3, we use a modified weighted round-robin scheduling to avoid grid congestion. In the following the number of MPCs will be denoted with M. For every time step, this scheduler receives the k-step ahead predictions of the inputs $u_{\text{i}}(k|t)$, $i \in \{1 : M\}, k \in \{t : t+N-1\}$ of each MPC i. It then uses these predictions to calculate a k-step ahead prediction of the grid constraints $u_{\text{sched, i}}(k|t)$, $i \in (1, M)$, $k \in \{t+1 : t+N-2\}$ for each MPC i as shown in Algorithm 1.

Algorithm 1: Modified weighted round robin scheduling of grid capacity u_{grid}.

Input : $u_{\text{grid}}, P_{\text{nom},i}, u_i(k|t), i \in \{1 : M\}, k \in \{1 : N\}$
Output: $u_{\text{sched},i}(k|t), i \in \{1 : M\}$
for $i \leftarrow 1$ **to** M **do**
  $w_i \leftarrow P_{\text{nom},i}/10000$;
  $o_i \leftarrow i$;
  $u_{\text{left},i} \leftarrow 0$;
end
for $k \leftarrow 1$ **to** N **do**
  $u_{\text{left, grid}} \leftarrow u_{\text{grid}}$;
  for $i \leftarrow 1$ **to** M **do**
    $u_{\text{left},i} \leftarrow u_{\text{left},i} + u_i(k|t)$;
    $u_{\text{sched},i}(k|t) \leftarrow 0$;
  end
  while $0 < u_{\textit{left, grid}}$ **do**
    for $i \leftarrow 1$ **to** M **do**
      if $0 < \sum_{i=1}^{M} u_{\textit{left},o_i}$ **then**
        if $0 < u_{\textit{left},o_i}$ **then**
          $t \leftarrow \min(w_{o_i}, u_{\text{left},o_i}, u_{\text{left, grid}})$;
          $u_{\text{sched},o_i} \leftarrow u_{\text{sched},o_i} + t$;
          $u_{\text{left},o_i} \leftarrow u_{\text{left},o_i} - t$;
          $u_{\text{left, grid}} \leftarrow u_{\text{left, grid}} - t$;
        end
      else
        $t \leftarrow \min(w_{o_i}, u_{\text{left, grid}})$;
        $u_{\text{sched},o_i} \leftarrow u_{\text{sched},o_i} + t$;
        $u_{\text{left, grid}} \leftarrow u_{\text{left, grid}} - t$;
      end
    end
    for $i \leftarrow 1$ **to** M **do**
      $o_i \leftarrow (o_i + 1) \bmod M$;
    end
  end
end

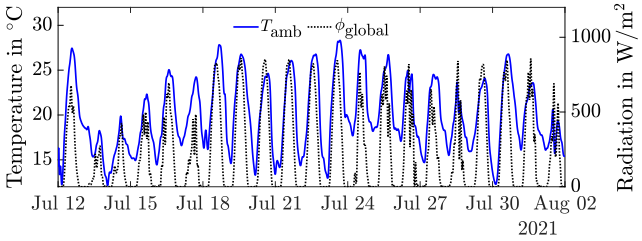

Fig. 3: Outside temperature and global solar radiation for the simulation period.

III. Evaluation

For the evaluation of the smart district model, we use input/output data resulting from a CityGML energy ADE [17]. The energy ADE enriches typical CityGML 3D building models with thermal energy related information for an EnergyPlus [18] simulation. Therefore, we also include reference temperature profiles and 2022 weather data from DWD [19] into the simulation. With the resulting time series of input/output data, we identify the grey-box model from Sec. II-B. This simulation data is used for potential analysis and could be replaced by real measured data of a smart district.

Next, we present the simulation results of the considered MPC formulations for a specific time range in summer 2021 (July 12 to August 2) when the outside temperatures were rather high. We use a prediction horizon of 8 h with a sampling period of 15 min for all our simulations. The disturbances during the simulation period are shown in Fig. 3. We use historical data from the German day-ahead electricity market as price signal [20], which we scale to $(0, 1)$. We assume perfect forecasts for all disturbances and the price signal. For a formulation including forecast uncertainties, we refer to [21]. To solve the optimization problems, we use CasADI [10].

The impact of the different scenarios on DR and thermal comfort performance is quantified in Tab. III with the Key Performance Indicators (KPI) [2]: Grid Costs (GC) and Mean Absolute Error (MAE):

$$\text{GC} = \sum_{i=1}^{M}\Big(\sum_{j=1}^{N} p_j \int_j u_j \, dt_j\Big)_i, \quad \text{MAE} = \frac{1}{N}\sum_{j=1}^{N} |\hat{y} - y_j| \,. \tag{11}$$

The GC are the sum of a product of the dynamic energy price p_i and used energy $\int_i u_i \, dt_i$ over the entire evaluation period with n steps for each building. The MAE is the difference between reference temperature $\hat{y}$ and actual air temperature y of each building. Superior performance is characterized by lower GC and lower MAE (temperature close to the reference of $\hat{y} = 21\,^{\circ}\text{C}$).

1. Decentralized MPC (DeMPC): First, we look at scenario 1 (see Fig. 1). Since every building gets the same price signal and the disturbances for all buildings are the same, they behave very similarly, as shown in Fig. 4. We note that air temperatures and cooling power demand are high during

TABLE III: Comparison of simulation results of different scenarios.

Scenario	Mean T_{air} (°C) / MAE (K)									Energy	GC
	Bldg 1	Bldg 2	Bldg 3	Bldg 4	Bldg 5	Bldg 6	Bldg 7	Bldg 8	Bldg 9	(MWh)	
DeMPC	21.92 / 1.32	21.65 / 1.24	21.56 / 1.27	21.64 / 1.25	21.70 / 1.25	21.90 / 1.30	21.76 / 1.30	21.48 / 1.32	21.49 / 1.27	122.4	72.40
CeMPC	21.87 / 1.31	21.65 / 1.25	21.52 / 1.27	21.61 / 1.25	21.67 / 1.25	21.75 / 1.27	21.68 / 1.29	21.39 / 1.32	21.49 / 1.27	126.0	77.89
DiMPC	21.69 / 1.21	21.62 / 1.22	21.49 / 1.25	21.59 / 1.22	21.64 / 1.22	21.64 / 1.21	21.59 / 1.22	21.41 / 1.29	21.51 / 1.26	128.0	78.95

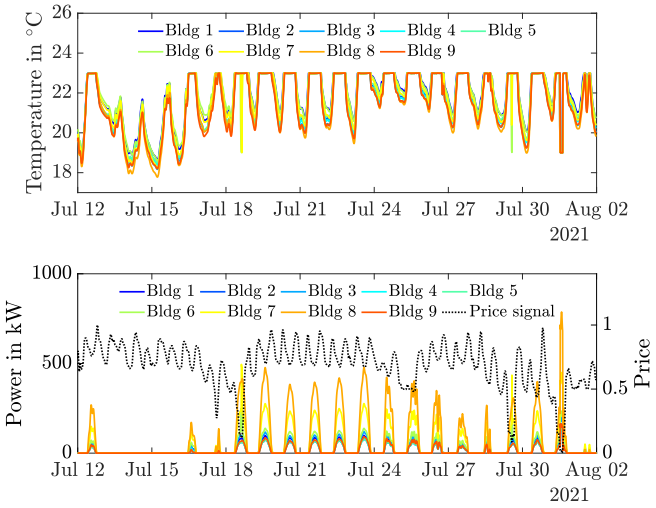

Fig. 4: DeMPC simulation results showing the temporal similarities of the different buildings' temperatures and cooling power demand.

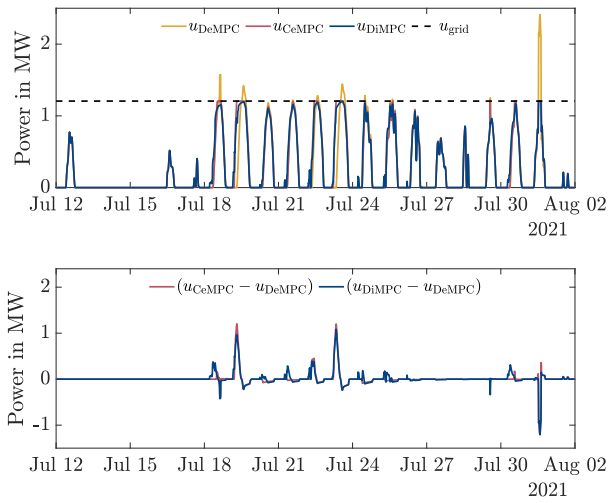

Fig. 5: Comparison of simulation results for all scenarios in regards to total cooling power demand.

the middle of each day except in the beginning from July 13 to July 15 when the outside temperatures are so low that additional cooling is not necessary. Furthermore, temperatures never exceed 23 °C and mean air temperature are well inside the acceptable range (see Tab. III). Nonetheless, we observe especially high power demand on July 31 when energy prices are at their lowest while the outside temperatures are high. We take this peak in demand as our baseline for the local grid's capacity which we try to reduce 50 % in scenarios CeMPC and DiMPC. This would allow the local grid to have some over-provisioning for the expected higher power demand due to more building cooling being installed in the future.

2. Centralized MPC (CeMPC): Next, we look at scenario 2 (see Fig. 1). As shown in Fig. 5 the total cooling power demand does not exceed the local grid limit $u_{\text{grid}} = 1.2\,\text{MW}$ but overall about 2.6 % more energy is needed resulting in a 7.6 % higher grid cost. Additionally, we observe slightly lower mean air temperatures as well as MAE for most buildings. These slightly lower mean air temperatures and higher cooling energy demand mainly come from the earlier and longer cooling periods on July 19 and July 23, as shown in Fig. 5.

3. Scheduled Distributed MPC (DiMPC): Lastly, looking at scenario 3 (see Fig. 1), we also see that the total cooling power demand does not exceed the local grid limit $u_{\text{grid}} = 1.2\,\text{MW}$, as shown in Fig. 5. The mean air temperatures are well inside the acceptable range, even slightly lower than in scenario 2. Then again, about 4.5 % more energy is needed than in scenario 1, resulting in a 9.0 % higher grid cost.

In summary, while DeMPC with DR is prone to cause grid congestion in the local electricity grid, both CeMPC and DiMPC are able to avoid grid congestion. We show that CeMPC and DiMPC can be applied to keep the total cooling power beneath a given maximum value while providing similar levels of thermal comfort, albeit causing a little increase in cooling energy demand (2.6 % more for CeMPC and 4.5 % for DiMPC) and providing slightly less DR as indicated by the 7.6 % and 9.0 % higher GC for CeMPC and DiMPC, respectively.

IV. Conclusion

In the present paper, we show that Decentralized MPC with Demand Response (DR) leads to a synchronous response of all buildings and results in a peak load that may burden the local power grid. To reduce this synchronous peak, we present two possible solutions, Centralized MPC and scheduled Distributed MPC. This can avoid possible grid congestion by considering an explicit grid limit for the total cooling power of all buildings.

For detailed evaluation, we present a baseline Decentralized MPC scenario where every building in the district optimizes its cooling power with regards to DR. In that baseline case, we observe a synchronous response from all the buildings (with a total maximum peak cooling power demand of about 2.4 MW). Because such peaks put high stress on the local

power grid of the district, we develop two additional Model Predictive Control (MPC) approaches that consider an explicit grid limit for the total cooling power of all buildings: Centralized MPC and Distributed MPC.

In the Centralized MPC, we solve one central optimization problem for all buildings and the local power grid. In the other approach, scheduled Distributed MPC, we add a central scheduler that communicates with the MPCs of each building and enforces the local power grid's constraints on maximum power. In both cases, our results yield a $50\,\%$ peak reduction of the total cooling power in the district, compared to the baseline case. We expect that the importance of these approaches will rise in the upcoming years due to the increasing cooling demand.

Acknowledgment

This work was conducted within the projects FlexKälte and SEKO, which are funded by the German Federal Ministries for Economic Affairs and Climate Action (BMWK) and Education and Research (BMBF). The authors would like to thank their colleagues from the Energy Lab 2.0 and the Institute for Automation and Applied Informatics (IAI) for all the fruitful discussions and collaborations.

Author Contributions

Author contributions according to Contributor Roles Taxonomy (CRediT, https://www.casrai.org/credit.html): *Conceptualization:* P.Z., M.F.; *Methodology:* P.Z., M.F.; *Software:* P.Z.; *Formal analysis:* P.Z.; *Investigation:* P.Z.; *Data curation:* K.-H.H.; *Writing - original draft:* P.Z., M.F., J.G.; *Writing - review and editing:* P.Z., M.F., J.G., K.-H.H., S.W., V.H:; *Visualization:* P.Z., M.F.; *Supervision:* S.W., H.M., V.H.; *Project administration:* H.M.; *Funding acquisition:* V.H.

References

[1] M. Larsen, S. Petrović, A. Radoszynski, R. McKenna, and O. Balyk, "Climate change impacts on trends and extremes in future heating and cooling demands over europe," *Energy and Buildings*, vol. 226, p. 110 397, 2020. DOI: https://doi.org/10.1016/j.enbuild.2020.110397.

[2] M. Frahm, P. Zwickel, J. Wachter, *et al.*, "Occupant-Oriented Economic Model Predictive Control for Demand Response in Buildings," in *Thirteenth ACM International Conference on Future Energy Systems*, Association for Computing Machinery, 2022. DOI: 10.1145/3538637.3538864.

[3] G. Coccia, A. Mugnini, F. Polonara, and A. Arteconi, "Artificial-neural-network-based model predictive control to exploit energy flexibility in multi-energy systems comprising district cooling," en, *Energy*, vol. 222, pp. 119 958–, 2021. DOI: 10.1016/j.energy.2021.119958.

[4] S. Buffa, A. Soppelsa, M. Pipiciello, G. P. Henze, and R. Fedrizzi, "Fifth-Generation District Heating and Cooling Substations: Demand Response with Artificial Neural Network-Based Model Predictive Control," en, *Energies*, vol. 13, no. 17, p. 4339, Aug. 2020. DOI: 10.3390/en13174339.

[5] J. Ma, S. J. Qin, B. Li, and T. Salsbury, "Economic model predictive control for building energy systems," in *ISGT 2011*, Jan. 2011, pp. 1–6. DOI: 10.1109/ISGT.2011.5759140.

[6] M. Mork, A. Xhonneux, and D. Müller, "Nonlinear Distributed Model Predictive Control for multi-zone building energy systems," *Energy and Buildings*, vol. 264, p. 112 066, 2022. DOI: https://doi.org/10.1016/j.enbuild.2022.112066.

[7] R. El Geneidy and B. Howard, "Contracted energy flexibility characteristics of communities: Analysis of a control strategy for demand response," en, *Applied Energy*, vol. 263, p. 114 600, Apr. 2020. DOI: 10.1016/j.apenergy.2020.114600.

[8] P. Pflaum, M. Alamir, and M. Y. Lamoudi, "Comparison of a primal and a dual decomposition for distributed MPC in smart districts," Nov. 2014, pp. 55–60. DOI: 10.1109/SmartGridComm.2014.7007622.

[9] H. Cai, C. Ziras, S. You, R. Li, K. Honoré, and H. W. Bindner, "Demand side management in urban district heating networks," en, *Applied Energy*, vol. 230, pp. 506–518, Nov. 2018. DOI: 10.1016/j.apenergy.2018.08.105.

[10] J. A. E. Andersson, J. Gillis, G. Horn, J. B. Rawlings, and M. Diehl, "CasADi – A software framework for nonlinear optimization and optimal control," *Mathematical Programming Computation*, vol. 11, no. 1, pp. 1–36, 2019. DOI: 10.1007/s12532-018-0139-4.

[11] P. Zwickel, A. Engelmann, L. Gröll, V. Hagenmeyer, D. Sauer, and T. Faulwasser, "A Comparison of Economic MPC Formulations for Thermal Building Control," in *2019 IEEE PES Innovative Smart Grid Technologies Europe (ISGT-Europe)*, 2019, pp. 1–5. DOI: 10.1109/ISGTEurope.2019.8905593.

[12] J. Koeln, B. Keating, A. Alleyne, C. Price, and B. P. Rasmussen, "Multi-zone temperature modeling and control," in *Intelligent Building Control Systems: A Survey of Modern Building Control and Sensing Strategies*, J. T. Wen and S. Mishra, Eds. Springer International Publishing, 2018, pp. 139–166. DOI: 10.1007/978-3-319-68462-8_6.

[13] M. Frahm, F. Langner, P. Zwickel, J. Matthes, R. Mikut, and V. Hagenmeyer, "How to Derive and Implement a Minimalistic RC Model from Thermodynamics for the Control of Thermal Parameters for Assuring Thermal Comfort in Buildings," in *Open Source Modelling and Simulation of Energy Systems (OSMSES)*, IEEE, 2022. DOI: 10.1109/OSMSES54027.2022.9769134.

[14] H. Harb, N. Boyanov, L. Hernandez, R. Streblow, and D. Müller, "Development and validation of grey-box models for forecasting the thermal response of occupied buildings," *Energy and Buildings*, vol. 117, pp. 199–207, 2016. DOI: 10.1016/j.enbuild.2016.02.021.

[15] The MathWorks Inc. "System Identification Toolbox - Create linear and nonlinear dynamic system models from measured input-output data." (accessed: 03.05.2022). (2022), [Online]. Available: https://mathworks.com/help/ident/.

[16] M. Frahm, E. Klumpp, S. Meisenbacher, J. Matthes, R. Mikut, and V. Hagenmeyer, "Development and Validation of Grey-Box Multi-Zone Thermal Building Models," in *BauSIM2022 - 9. Deutsch-Österreichische IBPSA-Konferenz: Tagungsband*, International Building Performance Simulation Association, 2022.

[17] A. Geiger, J. Benner, K.-H. Häfele, and V. Hagenmeyer, "Thermal energy simulation of buildings based on the citygml energy application domain extension," in *BauSIM2018 - 7. Deutsch-Österreichische IBPSA-Konferenz: Tagungsband*, International Building Performance Simulation Association, 2018, pp. 295–302.

[18] D. B. Crawley, L. K. Lawrie, F. C. Winkelmann, *et al.*, "Energyplus: Creating a new-generation building energy simulation program," *Energy and Buildings*, vol. 33, no. 4, pp. 319–331, 2001, Special Issue: BUILDING SIMULATION'99. DOI: https://doi.org/10.1016/S0378-7788(00)00114-6.

[19] Deutscher Wetterdienst. "Weather data in Karlsruhe, Germany." last accessed: 02.05.2022. (2022), [Online]. Available: https://www.dwd.de/.

[20] Bundesnetzagentur. "SMARD Strommarktdaten." (accessed: 26.01.2022). (2022), [Online]. Available: https://www.smard.de/home/downloadcenter/download-marktdaten.

[21] F. Oldewurtel, A. Parisio, C. Jones, *et al.*, "Use of model predictive control and weather forecasts for energy efficient building climate control," *Energy and Buildings*, vol. 45, pp. 15–27, Feb. 2012. DOI: 10.1016/j.enbuild.2011.09.022.